11B.4

TRENDS OF TROPICAL CYCLONE-INDUCED EXTREME PRECIPITATION IN EAST ASIA AND THEIR CAUSES

Cheuk Ki Jack Law*, Gabriele C Hegerl†, Nicolas Freychet‡
University of Leeds, University of Edinburgh†‡*

1. INTRODUCTION

Tropical cyclones (TCs) cause significant damage through strong winds, heavy precipitation and storm surges. There has been an observed increase in precipitation in TCs. The Clausius-Clapeyron relation relates a 1°C increase in temperature to a 7% of increase in precipitation rate. Some regions experience a higher rate of increase, for instance a 15% increase is observed in the US Gulf Coast (Van Oldenborgh et al. 2017). East Asia faces the Western North Pacific, which is the most active TC basin in the world. There is a need to understand the changes in extreme rainfall over the region to prepare us for the worst.

2. METHODS

The Asian Precipitation - Highly-Resolved Observational Data Integration Towards Evaluation (APHRODITE) dataset and the TC best track data from the Joint Typhoon Warning Center are used for this study from 1951 to 2015. We consider precipitation to be TC-related if the TC is within 800 km of a grid point in the region, and that to be extreme if it exceeds the 95th percentile. Our analysis focuses on coastal regions. We categorise the 12 regions as shown in figure 1, also further categorising those 12 regions into 5 large regions as follows:

- Western regions: South Vietnam, North Vietnam, Hainan and Zhanjiang, South China, Southeast China
- Eastern regions: North Philippines, South Philippines, East China, Taiwan, Korea, South Japan, North Japan
- Southern regions: North Philippines, South Philippines, South Vietnam, North Vietnam, Hainan and Zhanjiang
- Central regions: South China, Southeast China, East China, Taiwan
- Northern regions: Korea, South Japan, North Japan

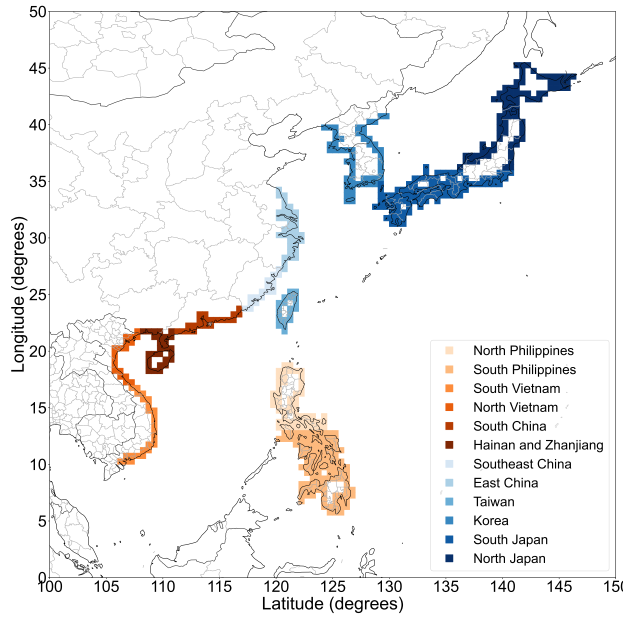

FIG. 1. The figure shows the grid squares that fall into the 12 costal regions.

2.1. Calculation

The workflow of the spatial extent and temporal extent follows the steps below:

i. Extract information on intense rainfall and TC location for each grid point

ii. Calculation of total TCEP on **each** grid point per TC during passage

iii. Averaging TCEP on **all** coastal grid points in the region (see figure 1)

iv. Averaging TCEP per event on all regions **per year**

v. Averaging TCEP on all large regions

We define two important periods: 1951–1978 (pre-satellite era) and 1979–2015 (satellite era). Satellites are useful in accurately tracking TCs to overcome the limitations imposed by the lack of observations over open ocean (Barcikowska et al. 2012).

The first step is to take the value of rainfall in each grid point and calculate the distance between the TC and the grid point. If the TC is within 800 km of the grid point over any of the tracked period, the rainfall is saved and the next step commences. To match the timestep of both datasets, we repeat the rainfall measurement 4 times each day to match the 6-hour interval of best track

*Corresponding author address: Priestley Building, University of Leeds, Woodhouse, Leeds, LS2 9JT
E-mail: eeckjl@leeds.ac.uk.
†Corresponding author address: Crew Building, The King's Buildings, Alexander Crum Brown Road, Edinburgh EH9 3FF
E-mail: gabi.hegerl@ed.ac.uk.
‡Corresponding author address: Crew Building, The King's Buildings, Alexander Crum Brown Road, Edinburgh EH9 3FF
E-mail: nicolas.freychet@ed.ac.uk.

data. Below outlines the detailed method of the calculation of the parameters:

- The total TCP during storm passage is the sum of the daily rainfall during the storm passage.
- The genesis location of the TC is the centre location of the TC at which it is first classified as a tropical depression.
- The maximum value of the TC intensity during the storm passage is finding the highest wind intensity at which the storm is within 800 km from the grid point.
- The number of days the TC takes to pass within 800 km of the point is the length of the precipitation array that contains rainfall amount at 6-hr intervals and divide it by 4, since there are 4 such measurements per day. The precipitation array can be substituted by other arrays having the same length since this is basically the number of measurements divided by 4.
- The mean TC translation speed during the storm passage is the arithmetic mean of the TC translation speed (distance between current location and previous location divided by 6 hours) during the storm passage to give absolute TC speed.

After making calculations for each TC and grid point, we take the arithmetic mean for the total TCP, TC genesis location, TC passage time and TC translation speed for all the grid points within the region, while we take the maximum value for the TC intensity for all the grid points within the region. The total TCP is considered TCEP if the maximum recorded daily rainfall during the storm's passage is larger than the 95th percentile on any day.

After that, we find out whether the region experiences TCEP by counting the number of grid points within the region experiencing TCEP during an event. If there are at least half of the grid points recording TCEP, the region is considered to have been affected by a TCEP event.

Finally, we aggregate results across the calendar year. We obtain results from the following parameters per year:

- Number of TCs passing through the region (passage frequency)
- Number of TCEP events in the region

and for each storm that produces TCEP we calculate:

- Average latitude and longitude of the genesis location of the TC
- Average maximum intensity of the TC
- Average number of days the TC takes to pass within 800 km of the region
- Average translation speed of the TC
- Average total TCP intensity in the region from the TC

Below outlines the detailed method of the calculation of the parameters:

- The number of TCEP events in the region is the aggregation of the number of TCEP events in the region per year.
- The number of TCs passing through the region each year is the total number of TCs that pass at least one grid point of the region each year.
- The average latitude and longitude of the genesis location of the TC which produces TCEP is the arithmetic mean of the average latitude and longitude of the TCs which produce TCEP events in the region, ruling out the TCs that do not produce TCEP. This is averaged each year.
- The average maximum intensity of the TC which produces TCEP is the arithmetic mean of the TC maximum wind intensity where the TCs produce TCEP events in the region, ruling out the TCs that do not produce TCEP. This is averaged each year.
- The average number of days the TC which produces TCEP takes to pass within 800 km of the region is the arithmetic mean of the passage time of the TCs that produce TCEP per year.
- The average translation speed of the TC which produces TCEP is the arithmetic mean of the translation speed of the TCs that produce TCEP events per year.
- The average total TCP intensity in the region from the TC is the arthimetic mean of the total TCP of the region that is considered TCEP.

To calculate the trend, we use the weighted least squares method to account for errors in the precipitation dataset and derive the significance using the two-tailed p-value from the Student's t-test.

We also calculate the Clausius-Clapeyron rate for comparison. First, we take the average temperature anomaly in East Asia and each large region. Then, we extrapolate the apparent rainfall intensity each year by using the Clausius-Clapeyron relation to derive the rainfall amount with relation to the temperature anomaly of that year, initialised using the rainfall amount of the first year in the best-fit slope of rainfall intensity.

3. RESULTS

The TCEP intensity and frequency have significantly increased by 33% and 39% respectively since 1951 (figure 2). Results for each large region are displayed in figures 3 and 4. The increase in intensity is larger than the background Clausius-Clapeyron, indicating other processes other than background warming contributing to a faster rate of increase. Meanwhile, the increase in frequency is noisy with a similar 95% confidence interval as the trend value. To reduce the noise, we normalise the TCEP frequency against the TC approach frequency to show the TCEP frequency fraction, which is done by dividing the TCEP frequency by the TCEP approach count. The results are presented in table 1, which indicate a significant increase overall.

To find the drivers of the increases in TCEP intensity and frequency, we analyse the TC properties, and internal and climate variability. Table 2 shows the abbreviation list of the factors that is displayed in figures 5 and 6. From figure 5, the changes in TCEP intensity can be attributed to the slowdown of TCs, northward and westward shift of TCs and background warming, while the changes in TCEP frequency can be attributed to TC passage frequency and the Pacific Decadal Oscillation (PDO) index. However, upon further investigation by using regression analysis in figure 7, the effects of PDO cannot explain the changes in TCEP frequency. Future research is needed to account for the effect of internal variability on TCEP frequency.

4. CONCLUSION

We conclude that there is a significant increase in TCEP intensity at a rate stronger than Clausius-Clapeyron scaling. This can be explained by both the direct thermodynamic effects of regional warming and a decrease in TC translation speed. There is also a significant increase in TCEP frequency with non-negligible noise, possibly moderated by the PDO and regional warming.

The West Pacific Subtropical High (WPSH) provides the steering flow for TCs in the West North Pacific basin. WPSH has been found to be influenced by global warming (He et al. 2015) and PDO (Liu and Chan 2008). The warming of the climate and negative PDO leads to the weakening and eastward retreat of WPSH, reducing the steering flow as TCs take a more northerly track, which is in line with the observed decreasing trend of TC translation speed and the northward and westward migration of TCs. Future targeted modelling studies should be undertaken to explain the link between climate warming and its effects on atmospheric circulation.

Acknowledgments. The authors would like to thank JTWC for providing the historical b-deck data that enable us to track past TCs with ease, and the providers of APHRODITE and REGEN for their work in collating the rainfall data so that the project is able to happen. GH and NF acknowledge the support of the NERC project EMERGENCE (NE/S004645/1) and GH was further supported by NERC project GloSAT (NE/S015698/1).

REFERENCES

Barcikowska, M., F. Feser, and H. Von Storch, 2012: Usability of best track data in climate statistics in the western north pacific. *Monthly weather review*, **140 (9)**, 2818–2830.

He, C., T. Zhou, A. Lin, B. Wu, D. Gu, C. Li, and B. Zheng, 2015: Enhanced or weakened western north pacific subtropical high under global warming? *Scientific reports*, **5 (1)**, 1–7.

Liu, K. S., and J. C. Chan, 2008: Interdecadal variability of western north pacific tropical cyclone tracks. *Journal of Climate*, **21 (17)**, 4464–4476.

Van Oldenborgh, G. J., and Coauthors, 2017: Attribution of extreme rainfall from hurricane harvey, august 2017. *Environmental Research Letters*, **12 (12)**, 124 009.

TABLE 1. The table shows the change in the TCEP frequency fraction since 1979 (the T40m slope value of the TCEP frequency fraction) and the corresponding Pearson correlation coefficients (corr) with surface air temperature anomaly and the PDO index. Values in parenthesis indicate the p-value with bolded values denoting 95% statistical significance.

Regions	40-year change	Temperature corr	PDO corr
Basin-wide	7.5% (**0.005**)	0.40 (**0.014**)	-0.38 (**0.022**)
West	8.2% (0.055)	0.21 (0.20)	-0.12 (0.47)
East	7.6% (**0.005**)	0.40 (**0.014**)	-0.49 (**0.002**)
South	6.5% (0.088)	0.11 (0.54)	-0.35 (**0.036**)
Central	10.8% (**0.011**)	0.43 (**0.008**)	-0.16 (0.35)
North	4.2% (0.31)	0.31 (0.062)	-0.31 (0.065)

TABLE 2. Potential drivers explaining the changes in TCEP intensity and frequency

Abbreviation	Full description
$\bar{\phi}$	Average latitude of all TC tracks
$\bar{\lambda}$	Average longitude of all TC tracks
ϕ_G	Regional average genesis latitude
λ_G	Regional average genesis longitude
f_A	Regional average TC passage frequency
f_B	Annual total number of TCs
I	Regional average TC wind intensity
t_P	Regional average number of days of TC passage within 800 km
v	Regional average TC translation speed
O_E	ENSO index
O_P	PDO index
O_J	Pacific-Japan teleconnection index
T	Surface air temperature anomaly

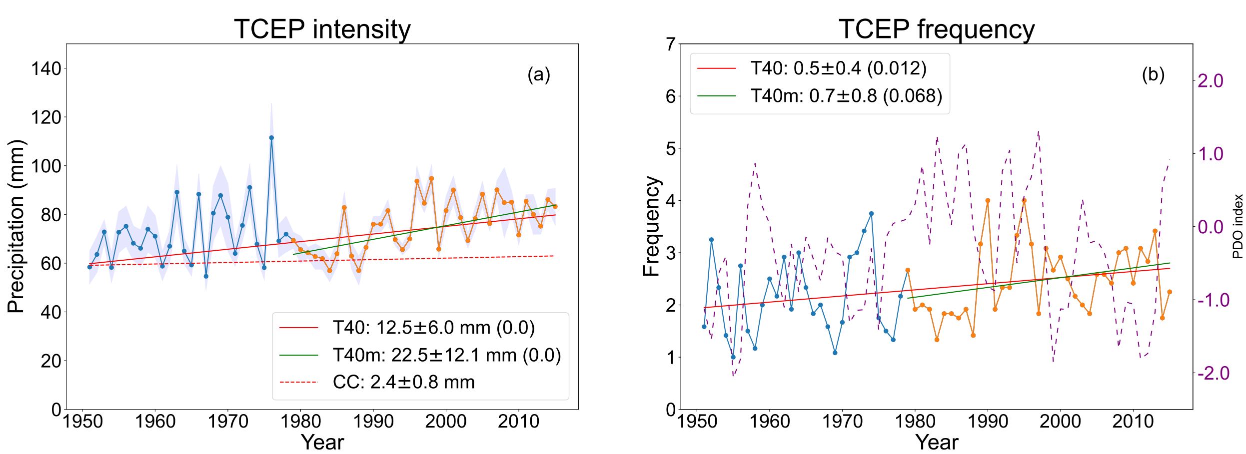

FIG. 2. Observed change in intensity (a) and frequency (b) of intense TC precipitation, overlain by the Clausius-Clapeyron slope and PDO index for comparison.

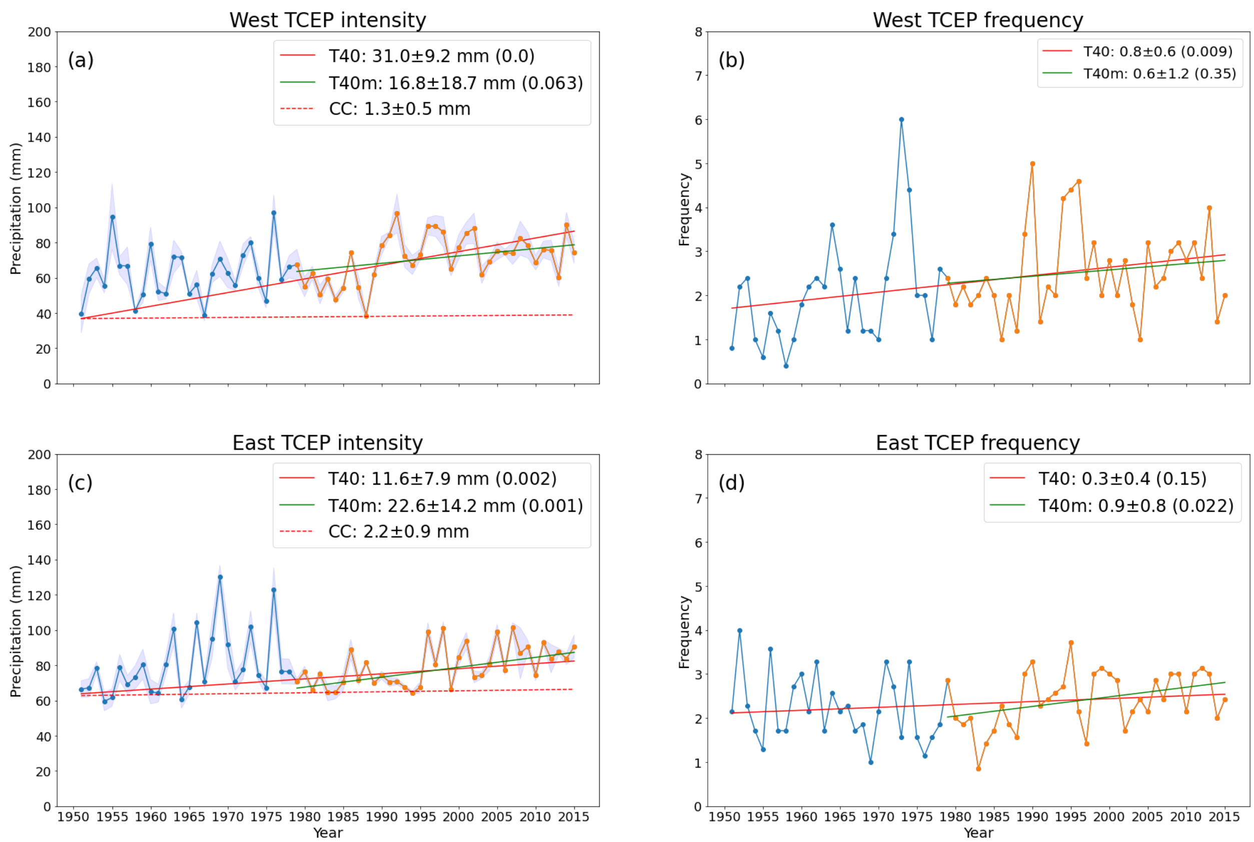

FIG. 3. Same as figure 2 but with west and east large regions

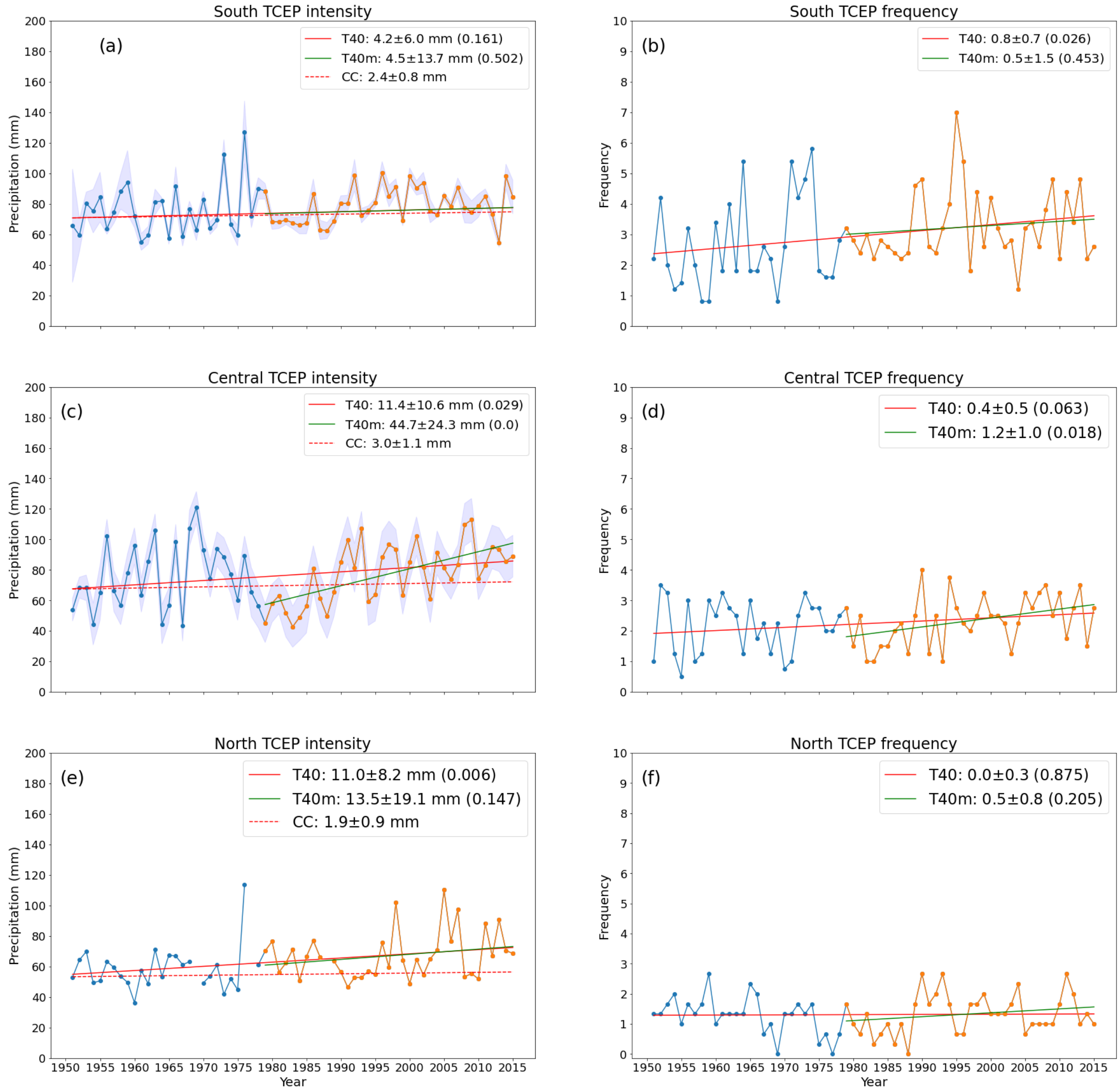

FIG. 4. Same as figure 2 but with north, central and south regions

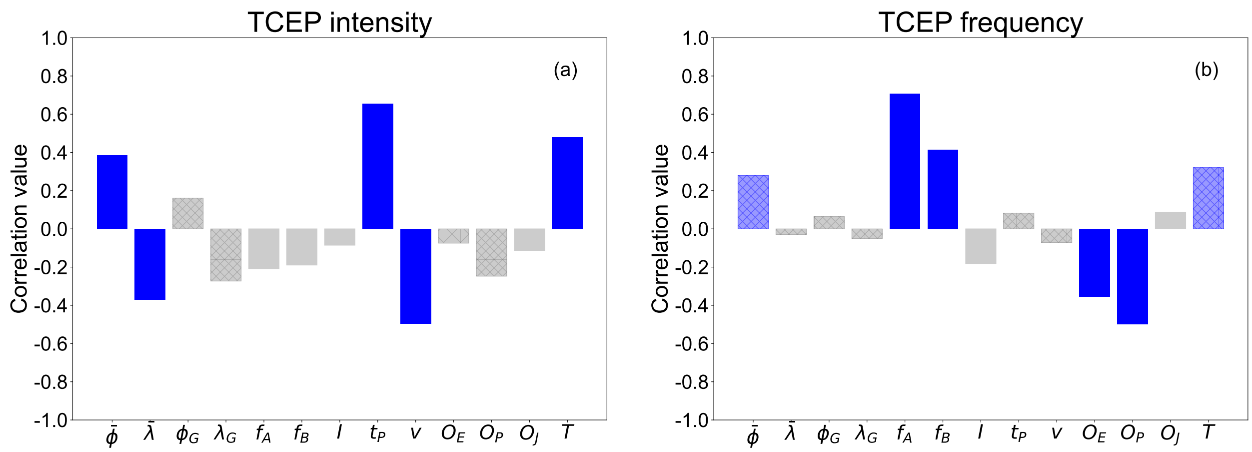

FIG. 5. Correlation of TCEP (a) intensity and (b) frequency with different possible drivers (see Table 2 for the detailed name of the abbreviations). 95% significance is indicated by dark opaque blue bars. Cross-hatching represents the corresponding trend of the driver is increasing (decreasing) with increasing TCEP (a) intensity and (b) frequency for positive (negative) correlation values with 95% statistical significance.

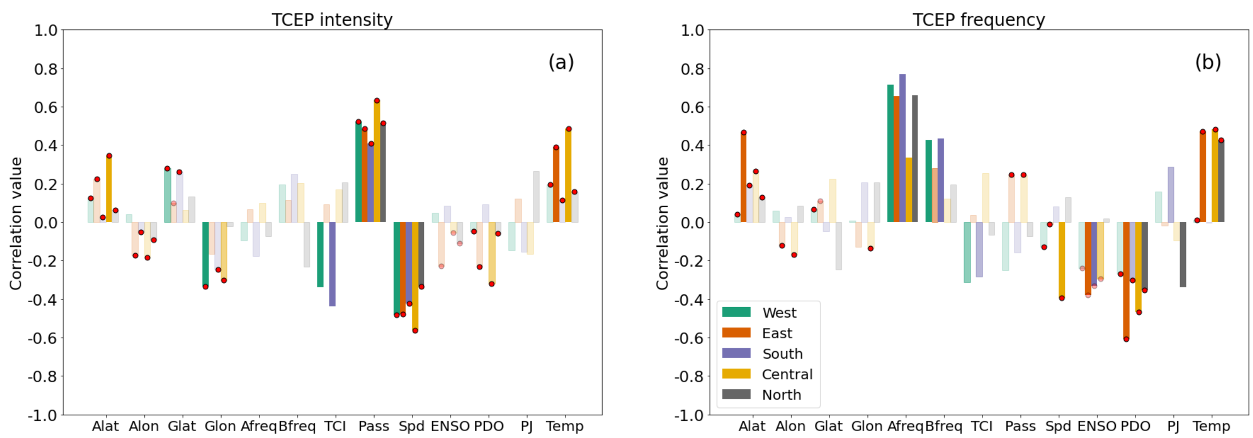

FIG. 6. Same as figure 5 but with all 5 large regions and red dot replacing cross-hatching

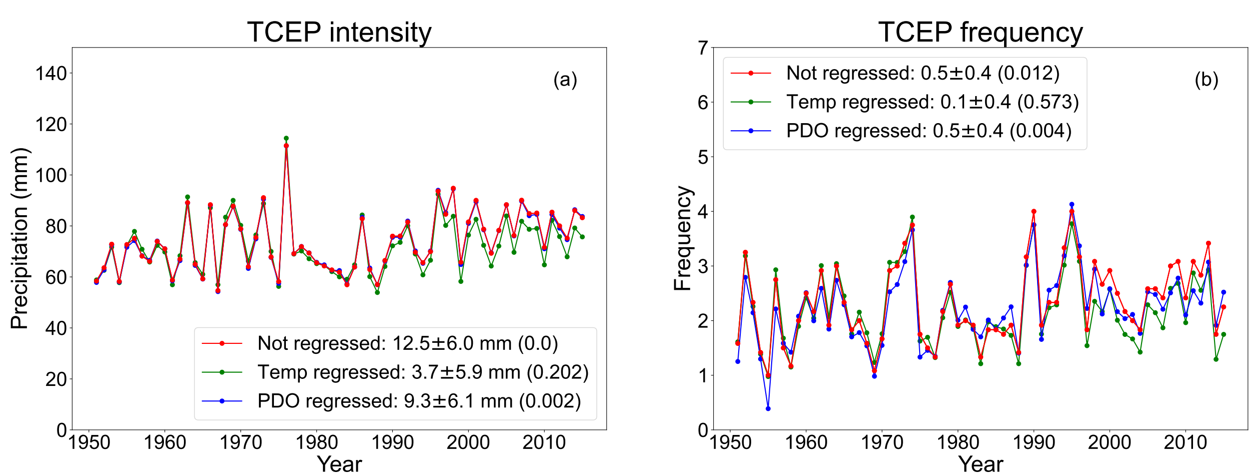

FIG. 7. Residuals of background and PDO derived from figure 2